TELKOMNIKA Telecommunication Computing Electronics and Control
Vol. 21, No. 5, October 2023, pp. 1147~1155
ISSN: 1693-6930, DOI: 10.12928/TELKOMNIKA.v21i5.24775

Reagentless iron detection in water based on unclad fiber optical sensor

Nurul Atika Nabila Jaharudin[1], Noran Azizan Cholan[1], Nurfatihah Che Abd Rashid[1], Nazrah Ilyana Sulaiman[1,2], Kim Gaik Tay[1], Nor Hafizah Ngajikin[1]
[1]Faculty of Electrical and Electronics Engineering, Universiti Tun Hussein Onn Malaysia (UTHM), 86400, Parit Raja, Batu Pahat, Johor, Malaysia
[2]Malaysia Marine and Heavy Engineering (MMHE), PLO3 Jalan Pekeliling, P.O Box 77, 81700 Pasir Gudang, Johor, Malaysia

Article Info

Article history:

Received Nov 08, 2022
Revised Jan 24, 2023
Accepted Feb 16, 2023

Keywords:

Fiber optical sensor
Iron detection
Unclad fiber

ABSTRACT

A simple and low-cost fiber based optical sensor for iron detection is demonstrated in this paper. The sensor head consist of an unclad optical fiber with the unclad length of 1 cm and it has a straight structure. Results obtained shows a linear relationship between the output light intensity and iron concentration, illustrating the functionality of this iron optical sensor. Based on the experimental results, the sensitivity and linearity are achieved at 0.0328/ppm and 0.9824 respectively at the wavelength of 690 nm. With the same wavelength, other performance parameters are also studied. Resolution and limit of detection (LOD) are found to be 0.3049 ppm and 0.0755 ppm correspondingly. This iron sensor is advantageous in that it does not require any reagent for detection, enabling it to be simpler and cost-effective in the implementation of the iron sensing.

Corresponding Author:

Noran Azizan Cholan
Faculty of Electrical and Electronics Engineering, Universiti Tun Hussein Onn Malaysia (UTHM)
86400, Parit Raja, Batu Pahat, Johor, Malaysia
Email: noran@uthm.edu.my

1. INTRODUCTION

Iron is one of the elements that exist naturally in water. A small amount of iron is essential to the body but high concentration of iron in water can cause it to have unpleasant taste, colour and odour. Meanwhile, in terms of health risk, excessive amount of iron in the body can lead to health problems such as disorder of iron metabolisms [1]. For this reason, World Health Organization (WHO) sets a guideline for iron concentration in drinking water being below than 0.3 ppm [2].

Traditionally, several methods have been introduced to detect iron concentration such as atomic absorption spectrometry (AAS) [3], [4] and inductively coupled plasma mass spectrometry (ICPMS) [5]. Apart from that, techniques of fluorescence [6], [7] and colourimetric [8], [9] have been also explored extensively. However, these methods require expensive instruments that needs to be operated by specialists, meaning that they are not suitable to be used in-situ [10]. Moreover, they requires complicated procedure for chemical preparation and therefore becomes difficult for the routine implementation [11].

On the other hand, fiber-based optical sensor approaches are now growing in various fields including chemical sensing owing to their unique properties like small in size, robust, low in cost, ability for remote sensing and immunity to the electromagnetic interference [12]. Typically, optical fiber based- chemical sensing can be done by modifying the structure of the fiber such as grating on the core (fiber bragg grating) [13], interferometer [14] and modified cladding [15], [16]. By modifying the cladding of the fiber, for instance the removal of cladding layer (unclad fiber), it can induce a few sensing phenomena such as surface plasmon resonance (SPR) and evanescent wave absorption (EWA).

In optical fiber-based SPR, a metallic layer is used to be deposited on the fiber core and forming a new cladding layer after the fiber cladding is removed. This metallic layer is used to generate surface plasmon wave (SPW) at fiber core-metal interface, as light from the fiber is incident on the metal surface [17]. Commonly, gold (Au) and silver (Ag) are employed in previous work [18] as the metallic layer due to their advantages of having a substantial amount of charge carriers and the suitability of sensing operation in the visible region spectrum [19]. As the technology of SPR emerges, a lot of new methods and materials have been explored to improve the sensitivity of SPR such as modifying the metal film by an overlayer of tungsten disulphide (WS2) nanosheets onto gold film [20] as well as utilizing dip-coated graphene over metals as in [21] and dip-coated graphene gold nanocomposite in [22].

Alternatively, for the unclad fiber to have interaction with that directly interacts with the liquid sensing medium, employment of EWA is another option. EWA occurs in the event of total internal reflection (TIR) in the core-cladding interface, where some of the energy escapes into the cladding medium and generates the electromagnetic field along the propagation referred as evanescent wave [23], [24]. Unlike the optical fiber-based SPR method that is highly complicated in fabrication, high in cost and sensitive to motion, EWA has advantages of simple fabrication, robustness and low cost [25].

According to the literature, there are many developments that utilize the principle of EWA by employing different types of unclad fiber structure [26]. For instance, straight (no bending), U-bent shape, D-shape and balloon-shape. For the straight structure, it offers simplicity and the fabrication process is less complicated in comparison with other structures [27]. Few developments have been reported regarding the use unclad fiber with straight structure for iron sensing [28]–[30]. Lee *et al.* [28] demonstrated a straight unclad fiber using both a multimode silica fiber and a multimode plastic fiber as the sensor head. The sample preparation of this work requires the addition of thiocyanate to the Fe^{3+} to deliver a red-coloured compounds. Meanwhile, Varghese *et al.* [29] demonstrated iron detection using a plastic multimode fiber. In this work, hydroxylamine hydrochloride and bathophenanthroline was used to produce a red-ferrous complex. In addition, a straight geometry of unclad fiber was utilized as the sensing head using plastic clad silica (PCS) fiber in [30]. In this work, the reaction with potassium ferro cyanide solution causes the blue coloured Fe^{2+} complex to appear. The common things in research work [28]–[30] are that they use chemical reagent for iron sensing.

In this work, we present a simple fiber optic method by unclading the plastic optical fiber (POF) in a straight structure using chemical etching method. The unclad fiber causes the light from the core to have interaction with the iron when the fiber is dipped in the iron solution. This work requires no reagent or other chemicals for sample preparation. Therefore, it offers simplicity in the implementation as well as cost-effectiveness due to the avoidance of the reagent.

2. METHOD

The experimental setup to investigate the iron concentration in water based on optical fiber sensor is demonstrated in Figure 1. The experimental setup consists of a halogen light source from ocean optics (DH-mini light source), a POF as the sensor head and a spectrometer from ocean optics (HR4000CGUV-VIS) as the detector. This spectrometer is connected to a computer for output monitoring using OceanView software. As for the sensor head, the POF used in this experiment has a polymethyl methacrylate (PMMA) core with the core and cladding diameter of 980 µm and 20 µm thick, respectively. The refractive index of the POF is 1.492 for the core and 1.417 for the cladding.

With the 15 cm length of the POF, the sensor head is fabricated by removing the cladding of the fiber at the centre using a chemical etching method. There are 3 sensor heads being prepared with different unclad region lengths of 1 cm, 2 cm, and 3 cm in order to analyze which length gives high performance. Acetone, de-ionized water, and sandpaper are involved in this chemical etching method. The cladding of the fiber is removed by immersing the POF in the acetone solution for 10 seconds and then the unclad POF is quickly dipped into the de-ionized water to stop the acetone reaction towards the cladding of the fiber [31], [32]. Afterwards, the sandpaper is used to scrub the outer fiber surface that has soft milky-white layer formed by the reaction earlier.

In this work, the fiber sensor is tested with iron concentration from the iron standard solution (pure iron) and also with the real water sample. Figure 2(a) shows the sample of pure iron solution used in this experiment. The iron standard solution is obtained from a manufacturer Hach with concentration of 10 ppm. This solution is then diluted into lower concentration of 0.1, 0.2, 0.3, 0.4, 0.5, 0.6, 0.7, 0.8, 0.9, and 1.0 ppm. There are a total of 10 samples of iron solution all together, and they are diluted by adding them with a certain amount of de-ionized water based on the dilution calculation. As for the reference sample, de-ionized water is used due to non-existence of mineral ions within.

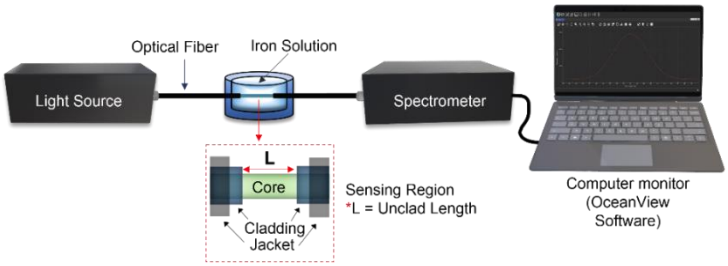

Figure 1. Experimental setup of fiber optic sensor

On the other hand, Figure 2(b) shows the real water sample with various amounts of iron concentration. The value of iron concentration is measured using a low range photometer, model HI97742 by Hanna Instrument. There are 5 samples of real water being used and their measured concentration are 0.24 ppm, 0.55 ppm, 0.97 ppm, 1.08 ppm and 1.6 ppm. As for the reference sample, de-ionized water is used for that purpose.

During the experiment, the sensor head is dipped into 10 ml of iron solution sample and the light intensity is observed in the computer through OceanView software. Data captured by the OceanView software is then extracted for the purpose of data analysis. The result for each iron sample solution is obtained by taking the average of 3 values during the measurement.

The method of detection in this work utilizes the principle of evanescent wave that occurs on the core-cladding interface. It is common knowledge that light propagation in the fiber is made possible due to the TIR. In this event, the incident angle is greater than the critical angle, causing light to reflect back from the core-cladding interface. However, at each TIR, a small amount of energy escapes and penetrates into the fiber cladding, creating an electromagnetic field called as the evanescent wave [23]. This evanescent wave is sensitive to the refractive index (RI) and consequently, whenever the sensor head is dipped into the sensing medium at different concentration, the evanescent could detect the changes accordingly.

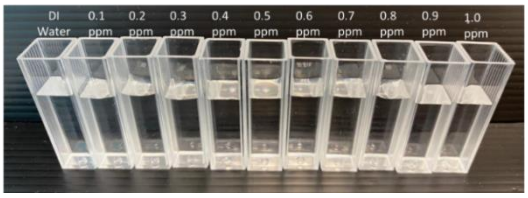

(a)

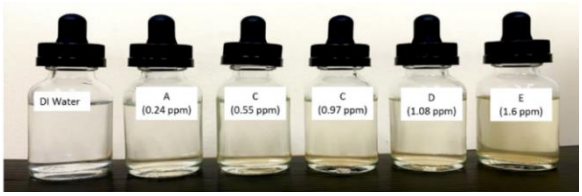

(b)

Figure 2. Variation of iron concentration in (a) iron standard solution and (b) real water samples

3. RESULTS AND DISCUSSION

Figure 3 demonstrates the light intensity output as the light passes through the plastic optical fiber at different unclad lengths. Based on the graph, it shows that the light intensity is about 10000 counts at 1 cm of unclad length, while at 2 cm and 3 cm of unclad length, the light intensity is about 6000 and 5000 counts respectively. Hence, it can be concluded that the light intensity decreases as the unclad length of the POF increases. This is expected as wider unclad length causes more light to escape from the core to the surrounding which leads to higher loss [33]. Therefore, this experimental work chooses the unclad length of 1 cm for the sensor head as it provides the highest output intensity, meaning that it has the lowest loss in comparison to other unclad lengths of 2 cm and 3 cm.

The output spectrum, shown in Figure 4, is the result of light intensity from the light source passing through the sensor head at different iron concentrations. Figure 4(a) shows the output spectrum in broader range of wavelength from 400 nm to 900 nm, while Figure 4(b) is for the narrow range of wavelength from 630 nm to 730 nm. The output spectrum at the narrow range is plotted to observe the behaviour of the peak wavelength at 690 nm as iron concentration varies. According to this result, it provides a linear trend of output light intensity as iron concentration increases. The unclad region from the sensor head causes the light from the core to leak to the surrounding and it has interaction with the iron solution. Due to the unclad structure of the POF in the sensor head, the iron solution therefore acts as a new cladding layer. Resulting from the increase of the sample refractive index with the iron concentration, the refractive index difference between the sample and fiber core reduces. Ultimately, the output light intensity increases as a consequence of the reduction of light loss.

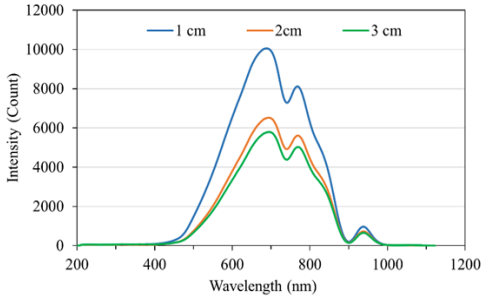

Figure 3. Output spectrum of light intensity at different unclad lengths

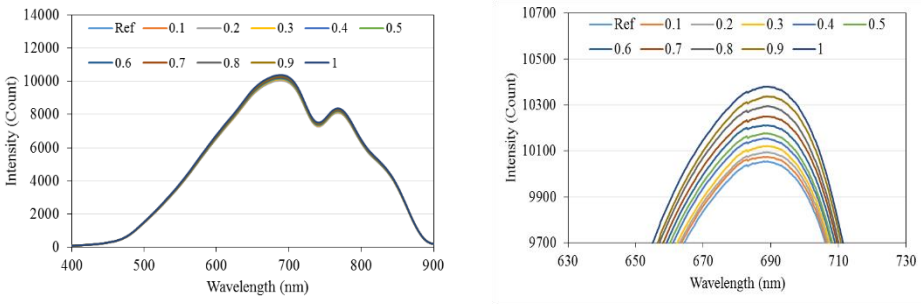

(a) (b)

Figure 4. Output spectrum as iron concentration varied: (a) at wavelength 400 nm to 900 nm and (b) at peak wavelength 690 nm

Several performance parameters are investigated in this research work, including the sensitivity and linearity of the sensor. The sensitivity and the linearity are analysed at two peak wavelengths which are 690 nm and 769 nm. Based on the result obtained illustrated in Figure 5, the sensitivity at 690 nm (0.0328/ppm) turned out to be slightly better than at 769 nm (0.031/ppm). On the other hand, the linearity performances at both wavelengths of 690 nm and 769 nm are 0.9824 and 0.9881 respectively. Both values are higher than 0.98, indicating that the relationship between the output light intensity and iron concentration is very much linear.

For futher investigation of other performance parameters, the wavelength is fixed at 690 nm as it has lower loss and better sensitivity in comparison to that at the wavelength of 769 nm. In this research work, the resolution of the sensor obtained is 0.3049 ppm which is calculated using the mathematical formula as [34]:

$$Resolution = \frac{N}{Sensitivity} \quad (1)$$

Where N, is the smallest scale of the detector (spectrometer) which is 0.01 while sensitivity is obtained through the slope of the graph earlier in Figure 5. Based on the formula, higher sensitivity results in lower resolution and resolution of the sensor basically indicates the smallest changes of the iron concentration that can be measured by the sensor.

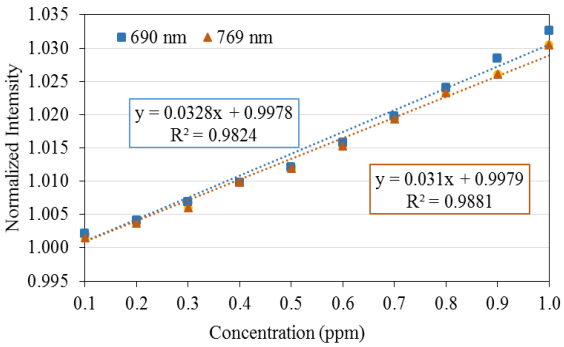

Figure 5. Performance analysis for sensitivity and linearity at wavelengths of 690 nm and 769 nm

In addition, the lowest iron concentration that can be detected by the sensor or also called as limit of detection (LOD) is obtained to be 0.0755 ppm which can be calculated using the formula as [34]:

$$LOD = \frac{3.3\ x\ \sigma}{S} \quad (2)$$

Where, σ is the standard deviation and S, is the sensitivity of the sensor.

Apart from that, the stability and stability precision of the sensor are studied and the result is presented in Figure 6. Figure 6(a) shows the output light intensity for over 180 seconds. Based on this result, the total fluctuation of light intensity attained is 32.08 count with the highest value of 10227.54 at 74 seconds and the lowest value of 10195.49 at 7 seconds. Whereas, Figure 6(b) shows the result of the stability precision plotted in one graph for iron concentration from 0.1 ppm to 1.0 ppm. The value obtained is within the range of 99.77% (lowest) and 99.91% (highest) at 1 ppm and 0.8 ppm correspondingly.

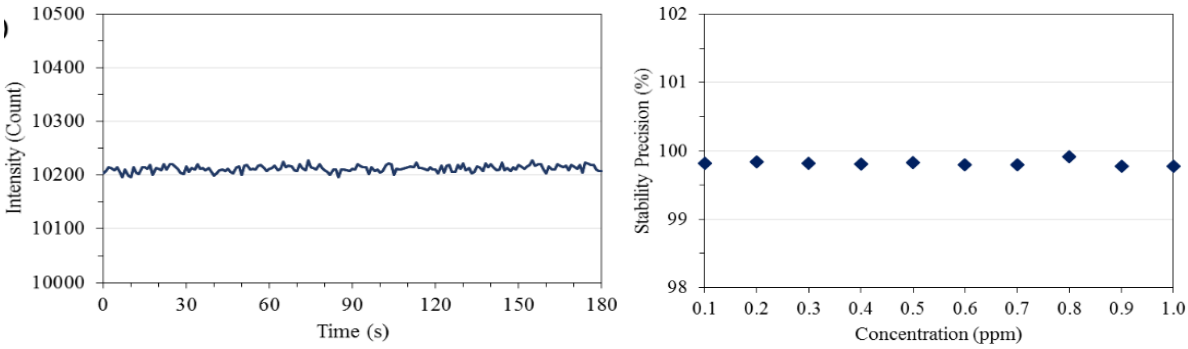

(a) (b)

Figure 6. Performance analysis of fiber optic sensor in term of (a) stability vs time and (b) stability precision

In this research work, the experiment is repeated for 3 times for every concentration. The measurement of the output result for these 3 experiments is recorded and plotted in the graph as shown in Figure 7. Based on this result, the relative standard deviation (RSD) is then calculated and presented in Figure 8. Since RSD is the ratio of the standard deviation, σ to the mean, μ value, hence the formula used in this research work to calculate RSD is given as in (3):

$$RSD = \frac{Standard\ deviation, \sigma}{Mean, \mu} \times 100 \quad (3)$$

Based on the result, the minimum RSD value obtained is 0.0019 at 0.9 ppm of iron concentration, while the maximum RSD value obtained is 0.0083 at 0.4 and 0.5 ppm of iron concentration. The calculated value for differences between maximum and minimum of RSD is obtained to be 0.0064. Based on the analysis of RSD value, we can conclude that this research work provides a precise measurement data as the RSD value is low, showing less data spreading.

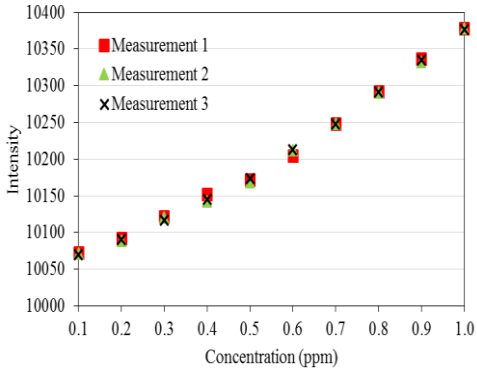

Figure 7. Relative standard deviation (RSD) over 3 times measurement

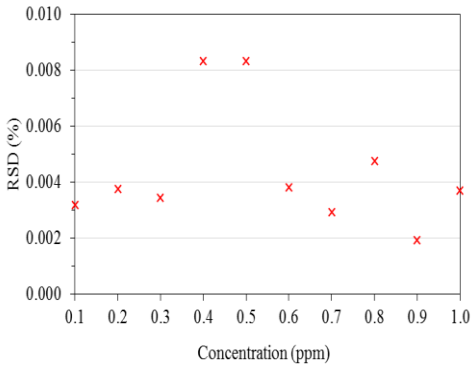

Figure 8. RSD value as concentration varies

In order to provide a thorough analysis, the same sensor head is tested with real water samples. As discussed in the earlier part, the wavelength used is 690 nm since it provides better sensitivity than 769 nm. Figure 9 shows the analysis of the result obtained through the experiment conducted for real water samples, the sensitivity and linearity obtained are 0.0091/ppm and 0.7904 respectively. With respect to these two performance parameters, it is evident that the result for real water samples is not as good in comparison to the result of iron standard solution. This is probably due to the existence of other chemicals in the real water samples and it may cause the interference effect, hence degrading the sensor performances.

In comparison with previous developments, this work demonstrates comparable performance for linearity but lower performance for sensitivity. With respect to operation, this proposed sensor has the edge in that it does not require reagent for the measurement, indicating the simplicity in the operation. The result comparison of this work and previous work is presented in Table 1.

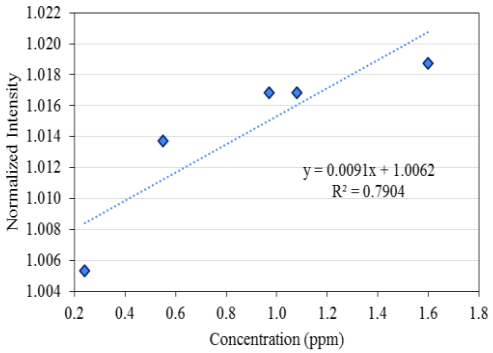

Figure 9. Analysis of real water samples as iron concentration varies

Table 1. Comparison with previous research work

References	Year	Structure	Sensitivity	R^2	Use of reagent
[28]	2003	Straight	–	–	Yes
[29]	2013	Straight	-0.1842/ppm	0.9959	Yes
[30]	2016	Straight	-0.0751/ppm	0.9453	Yes
This work	2022	Straight	0.0328/ppm	0.9824	No

For improvement, the sensitivity and selectivity of the sensor could be further enhanced in a few ways. For example, the optical fiber sensor could be fabricated with different geometry structure [35] and addition of coating layers to the sensor head in order to improve the sensitivity and selectivity of the sensor towards iron concentration. The geometry structure can help to improve the sensitivity via the increase of the penetration depth and the number of TIR events at shorter wavelengths [23]. Meanwhile, coating layer can help to improve the selectivity of the sensing medium and thus lowering the risk of interference effect.

4. CONCLUSION

In conclusion, an unclad optical fiber sensor for iron detection is successfully presented in this work. The sensing head is based on unclad fiber in which the light from the core leaks to the surrounding and interacts with the iron solution at different concentrations. For optimization of the unclad length, the unclad fiber is tested at 3 different lengths of 1 cm, 2 cm and 3 cm. The unclad length of 1 cm is chosen for the sensor head due to its lowest loss compared to others. The sensitivity and linearity obtained using this sensing head are 0.0328/ppm and 0.9824 respectively at the wavelength of 690 nm. In this work, the detection of the iron concentration does not require any chemical reagent, thus offering simplicity and cost-effectiveness to the sensing implementation.

ACKNOWLEDGEMENTS

The authors thank Universiti Tun Hussein Onn Malaysia (UTHM) for supporting this research work under Research Enhancement Graduate Grant (RE-GG) Code Q066. Communication of this research is made possible through monetary assistance by the UTHM Publisher's Office via Publication Fund E15216.

REFERENCES

[1] P. T. Lieu, M. Heiskala, P. A. Peterson, and Y. Yang, "The roles of iron in health and disease," *Molecular Aspects of Medicine*, vol. 22, no. 1–2, pp. 1–87, 2001, doi: 10.1016/S0098-2997(00)00006-6.

[2] Z. Yan, L. Hu, and J. You, "Sensing materials developed and applied for bio-active Fe3+ recognition in water environment," *Analytical Methods*, vol. 8, no. 29, pp. 5738–5754, 2016, doi: 10.1039/C6AY01502F.

[3] P. Liang, H. Sang, and Z. Sun, "Cloud point extraction and graphite furnace atomic absorption spectrometry determination of manganese(II) and iron(III) in water samples," *Journal of Colloid and Interface Science*, vol. 304, no. 2, pp. 486–490, 2006, doi: 10.1016/j.jcis.2006.09.006.

[4] G. Dima *et al.*, "Fe, Mn and Zn concentrations determination from Ialomipa River by atomic absorption spectroscopy," *Romanian Journal of Physics*, vol. 51, no. 5–6, pp. 667–674, 2006. [Online]. Available: https://www.researchgate.net/profile/Calin-D-Oros/publication/253575255_Fe_Mn_and_Zn_concentrations_determination_from_Ialomita_River_by_atomic_absorption_spectroscopy/links/5e3bddcb92851c7f7f201da1/Fe-Mn-and-Zn-concentrations-determination-from-Ialomita-River-by-atomic-absorption-spectroscopy.pdf

[5] G. L. Arnold, S. Weyer, and A. D. Anbar, "Fe isotope variation in natural materials measured using high mass resolution Multiple Collector ICPMS," *Analytical Chemistry*, vol. 76, no. 2, pp. 322–327, 2004, doi: 10.1021/ac034601v.

[6] X. Zhu, Y. Duan, P. Li, H. Fan, T. Han, and X. Huang, "A highly selective and instantaneously responsive Schiff base fluorescent sensor for the 'turn-off' detection of iron(III), iron(II), and copper(II) ions," *Analytical Methods*, vol. 11, no. 5, pp. 642–647, 2019, doi: 10.1039/C8AY02526F.

[7] S. O. Tümay, M. H. I.-Nezhad, and A. Khataee, "Development of dipodal fluorescence sensor of iron for real samples based on pyrene modified anthracene," *Spectrochimica Acta Part A: Molecular and Biomolecular Spectroscopy*, vol. 261, 2021, doi: 10.1016/j.saa.2021.120017.

[8] L. Lu, H. Yang, P. Guo, L. Xu, J. Huang, and J. Ma, "A novel rhodamine phosphorus derivative as fluorescent and colorimetric sensor for highly selective detection of Fe3+ in solution," *Optical Materials*, vol. 133, 2022, doi: 10.1016/j.optmat.2022.112767.

[9] X. Meng, B. Lei, N. Qi, and B. Wang, "The selective detection of Fe3+ ions using citrate-capped gold nanoparticles," *Analytical Biochemistry*, vol. 637, 2022, doi: 10.1016/j.ab.2021.114453.

[10] R. Kumar, M. Kachwaha, S. Verma, and D. Patidar, "Quick detection of iron in contaminated water before feeding to RO membranes," *SN Applied Sciences*, vol. 1, no. 427, 2019, doi: 10.1007/s42452-019-0379-6.

[11] A. Q. Alorabi, "A new colorimetric chemosensor based on 1,3,4-oxadiazole derivative for the high selectivity and sensitivity of Fe3+ ion detection," *Journal of Molecular Structure*, vol. 1251, 2022, doi: 10.1016/j.molstruc.2021.132019.

[12] H. D. Jahromi, "Performance analysis of transmissive modified cladding optical fibre sensors," *IET Optoelectronics*, vol. 16, no. 2, pp. 63–71, 2022, doi: 10.1049/ote2.12057.

[13] A. Boersma, R. Cremers, and R. Jansen, "Fiber Bragg Grating Distributed Chemical Sensors," *Procedia Engineering*, vol. 168, pp. 1245–1248, 2016, doi: 10.1016/j.proeng.2016.11.435.

[14] Pappa M, A. Mukherjee, and Elumalai R., "Design a sensor Mach Zender Interferometer for the detection of chemical and organic substances present in food and health drinks," *International Journal of Engineering and Advanced Technology (IJEAT)*, vol. 8, no. 6, pp. 4726–4730, 2019, doi: 10.35940/ijeat.F9226.088619.

[15] H. A. Mohammed, A. Almamori, and A. A. Alwahib, "Cladding modified fiber bragg grating for copper ions detection," *Semiconductor Science and Information Devices*, vol. 3, no. 2, pp. 12–16, 2021, doi: 10.30564/ssid.v3i2.3749.

[16] V. Kumar N., Kavitha BS, and S. Asokan, "Selective detection of lead in water using etched fiber Bragg grating sensor," *Sensors Actuators B Chemical*, vol. 354, 2022, doi: 10.1016/j.snb.2021.131208.

[17] M. N. Hossen, M. Ferdous, M. A. Khalek, S. Chakma, B. K. Paul, and K. Ahmed, "Design and analysis of biosensor based on surface plasmon resonance," *Sensing and Bio-Sensing Research*, vol. 21, pp. 1–6, 2018, doi: 10.1016/j.sbsr.2018.08.003.

[18] L. Singh *et al.*, "Gold nanoparticles and uricase functionalized tapered fiber sensor for uric acid detection," *IEEE Sensors Journal*, vol. 20, no. 1, pp. 219–226, 2020, doi: 10.1109/JSEN.2019.2942388.

[19] S. V. P. Radha, S. K. S. A. R. Nair, and S. S. Iyer, "Surface plasmon resonance-based fiber-optic metallic multilayer biosensors," *ACS Omega*, vol. 6, no. 23, pp. 15068–15077, 2021, doi: 10.1021/acsomega.1c01236.

[20] H. Wang *et al.*, "Sensitivity-enhanced surface plasmon resonance sensor utilizing a tungsten disulfide (WS_2) nanosheets overlayer," *Photonics Research*, vol. 6, no. 6, pp. 485-491, 2018, doi: 10.1364/PRJ.6.000485.

[21] M. Gomaa, A. Salah, and G. A. Fattah, "Utilizing dip-coated graphene/nanogold to enhance SPR-based fiber optic sensor," *Applied Physics A*, vol. 128, no. 56, 2022, doi: 10.1007/s00339-021-05196-z.

[22] M. Gomaa, A. Salah, and G. A. Fattah, "Superior enhancement of SPR fiber optic sensor using laser sensitized dip-coated graphene gold nanocomposite probes," *Optics & Laser Technology*, vol. 157, 2023, doi: 10.1016/j.optlastec.2022.108644.

[23] N. Punjabi, J. Satija, and S. Mukherji, "Evanescent wave absorption based fiber-optic sensor - cascading of bend and tapered geometry for enhanced sensitivity," in *Sensing Technology: Current Status and Future Trends III. Smart Sensors*, Springer,

Cham, CH, 2015, vol. 11, pp. 25–45 doi: 10.1007/978-3-319-10948-0_2.
[24] S. F. Memon, M. M. Ali, J. T. Pembroke, B. S. Chowdhry, and E. Lewis, "Measurement of ultralow level bioethanol concentration for production using evanescent wave based optical fiber sensor," *IEEE Transactions on Instrumentation and Measurement*, vol. 67, no. 4, pp. 780–788, 2018, doi: 10.1109/TIM.2017.2761618.
[25] K. Azil, K. Ferria, and S. Bouzid, "Cladless optical fiber sensor based on evanescent wave absorption for monitoring methylene blue induced water pollution," *Journal of the Optical Society of America B*, vol. 37, no. 11, pp. A253-A258, 2020, doi: 10.1364/JOSAB.396646.
[26] R. Jarzebinska, S. Korposh, S. James, W. Batty, R. Tatam, and S. -W. Lee, "Optical gas sensor fabrication based on porphyrin-anchored electrostatic self-assembly onto tapered optical fibers," *Analytical Letters*, vol. 45, no. 10, pp. 1279-1309, 2012, doi: 10.1080/00032719.2012.673097.
[27] A. K. Sharma, J. Gupta, and I. Sharma, "Fiber optic evanescent wave absorption-based sensors: A detailed review of advancements in the last decade (2007–18)," *Optik*, vol. 183, pp. 1008–1025, 2019, doi: 10.1016/j.ijleo.2019.02.104.
[28] S. T. Lee *et al.*, "Evanescent wave fibre optic sensors for trace analysis of Fe3+ in water," *Measurement Science and Technology*, vol. 14, no. 6, pp. 858–861, 2003, doi: 10.1088/0957-0233/14/6/322.
[29] B. P. Varghese, A. B. Pillai, and M. K. Naduvil, "Fiber optic sensor for the detection of ammonia, phosphate and iron in water," *Journal of Optics*, vol. 42, pp. 78–82, 2013, doi: 10.1007/s12596-013-0121-5.
[30] V. K. Kulkarni, H. H. Bendigeri, and R. M. Kulkarni, "LED based evanescent wave fiber optic sensor technique to detect Fe+2 concentration," *AIP Conference Proceedings*, vol. 1731, no. 1, 2016, doi: 10.1063/1.4947830.
[31] N. C. A. Rashid *et al.*, "Optimization of light source wavelength for ammonia detection in water," *TELKOMNIKA (Telecommunication Computing Electronics and Control)*, vol. 20, no. 5, pp. 1132–1138, 2022, doi: 10.12928/telkomnika.v20i5.24079.
[32] N. I. Sulaiman *et al.*, "Temperature sensing utilizing unclad plastic optical fiber with a balloon-like bent structure," *Applied Optics*, vol. 60, no. 13, pp. 3895–3900, 2021, doi: 10.1364/AO.419801.
[33] F. Abdurrahman, N. Arsad, S. Shaari, A. A. A. Bakar, and P. S. Menon, "Effects of cladding modification on the sensing potential of intrinsic polymer optical fiber as a VOCs sensor," *Journal of Optoelectronics and Advanced Materials*, vol. 17, no. 5–6, pp. 901–906, 2015. [Online]. Available: https://joam.inoe.ro/articles/effects-of-cladding-modification-on-the-sensing-potential-of-intrinsic-polymer-optical-fiber-as-a-vocs-sensor/
[34] A. Yaacob *et al.*, "Linearity range enhancement in direct detection of low concentration uric acid," *Optik*, vol. 249, 2022, doi: 10.1016/j.ijleo.2021.168243.
[35] M. Ashraf, Mainuddin, M. T. Beg, F. Moin, R. Rajesh, and G. Singhal, "U-bent plastic optical fiber sensor for iron in iron supplements," *IEEE Sensors Journal*, vol. 22, no. 15, pp. 14921–14928, 2022, doi: 10.1109/JSEN.2022.3187829.

BIOGRAPHIES OF AUTHORS

Nurul Atika Nabila Jaharudin received her Bachelor Degree in Electronic Engineering from Universiti Tun Hussein Malaysia (UTHM) in 2018. In the same year, she enrolled as Master Degree student in UTHM and her research field was fiber laser sensor. Currently, she is pursuing her studies in PhD, in electrical engineering from the same university. Her research interests include development of optical fiber sensors and optical communication. She can be contacted at email: n.atikanabila@gmail.com.

Noran Azizan Cholan is an Associate Professor in the Faculty of Electrical and Electronics Engineering at Universiti Tun Hussein Onn Malaysia. He received his Bachelor Degree in Electronics Engineering at Universiti Tenaga Nasional Malaysia in 2002. Afterwards in 2004, he obtained his Master Degree in Electronics-Telecommunications Engineering at Universiti Teknologi Malaysia. In 2015, he completed his PhD Degree at Universiti Putra Malaysia. During his PhD study, he went to Swansea University, UK and The Hong Kong Polytechnic University, Hong Kong for research attachment. As of now, he has been authors/co-authors for 69 journal conference proceeding papers. His research interests include lasers, amplifiers, optics modeling, microwave optics and optical sensors. He can be contacted at email: noran@uthm.edu.my.

Nurfatihah Che Abd Rashid received her B.E and M.E in Electrical Engineering from Universiti Teknologi Malaysia (UTM) in 2015 and 2019 respectively. She has involved in research on spectrophotometric detection for uric acid and soil nutrient applications. She is currently pursuing a PhD degree in Faculty of Electrical and Electronic Engineering, Universiti Tun Hussein Onn Malaysia (UTHM). She can be contacted at email: nurfatihahcar@gmail.com.

Nazrah Ilyana Sulaiman received her Bachelor Degree in Electrical and Electronic Engineering from Universiti Teknologi Malaysia (UTM). Currently, she is pursuing a part-time Masters degree in Faculty of Electrical and Electronic Engineering, Universiti Tun Hussein Onn Malaysia (UTHM) in the field of Optical Sensor application. Presently working at Malaysia Marine and Heavy Engineering (MMHE) as Mechanical Completion - Instrumentation Engineer, specialised in Field engineering, construction, installation, pre commissioning, Hook-Up & Commissioning and Start-Up of Topside platforms. She has completed a various Greenfield and Brownfield projects including onshore and offshore phases in Oil and Gas upstream industry with major clients namely PETRONAS , EXXONMOBIL, SHELL, TECHNIP, CHEVRON & AKER SOLUTIONS. She can be contacted at email: nazrahi.sulaiman@mmhe.com.my.

Kim Gaik Tay is an Associate Professor of Applied Mathematics in the Faculty of Electrical and Electronic Engineering at Universiti Tun Hussein Onn Malaysia. Her research interests include Nonlinear Waves, Optical Solitons, Fiber Optics Parametric Amplifier (FOPA), Numerical Methods, Forecasting, Breast Cancer Classification and Dorsal Hand Vein Pattern Recognition using machine learning and deep learning techniques. She completed her Bachelor's, Master and Ph.D. degrees in Applied Mathematics at Universiti Teknologi Malaysia. She is currently a member of the International Association of Engineers (IAENG) and Persatuan Sains Matematik Malaysia (PERSAMA). She can be contacted at email: tay@uthm.edu.my.

Nor Hafizah Ngajikin received her B.E and M.E in Electronic Engineering from Universiti Teknologi Malaysia (UTM) in 2001 and 2003 respectively. She was awarded a PhD from UTM for her work on MEMS Fabry-Perot optical tunable filter. From 2004 – 2017, she served as a senior lecturer and researcher at Lightwave Communication Research Group (LCRG), UTM. She is currently a lecturer at Universiti Tun Hussein Onn Malaysia. Her research interest includes an optical devices and sensors for biomedical applications. She can be contacted at email: norhafizah@uthm.edu.my.